ISSN: 2277-9655
Impact Factor: 4.116

IJESRT

INTERNATIONAL JOURNAL OF ENGINEERING SCIENCES & RESEARCH TECHNOLOGY

NUMERICAL SIMULATION OF TRUNCATED PYRAMIDAL CUPS OF AA1050-H18 ALLOY FABRICATED BY SINGLE POINT INCREMENTAL FORMING

V. Srija* and A. Chennakesava Reddy

* PG student Department of Mechanical Engineering, JNTUH College of Engineering, Hyderabad, Telangana, India

Professor, Department of Mechanical Engineering, JNTUH College of Engineering,Hyderabad, Telangana, India-chennakesava@jntuh.ac.in

DOI: 10.5281/zenodo.55981

ABSTRACT

The purpose of the present project work was to understand the formability of AA1050-H18 alloy to fabricate truncated pyramidal cups using single point incremental forming (SPIF) process. The finite element analysis has been carried out to model the single point incremental forming process using ABAQUS software code. The process parameters of SPIF were sheet thickness, step depth, tool radius and coefficient of friction. The process parameters have been optimized using Taguchi techniques. The major process parameters influencing the SPIF of truncated pyramidal cups were tool radius and coefficient of friction.

KEYWORDS: AA1050-H18 alloy, pyramidal cup, single point incremental forming, finite element analysis, step depth, tool radius, sheet thickness, coefficient of friction.

1. INTRODUCTION

Deep drawing process has been extended to fabricate variety of cups through plastic deformation of sheet material using dies. In a series of research on deep drawing process to fabricate variety of cup shapes, rich investigation have been carried out to improve the superplastic properties of materials such as AA1050 alloy [1], AA1070 alloy [2], AA1080 alloy [3], AA1100 alloy [4], AA2014 alloy [5], AA2017 alloy [6], AA2024 alloy [7], AA2219 alloy [8], AA2618 alloy [9], AA3003 alloy [10], AA5052 alloy [11], AA5039 alloy [12], Ti-Al-4V alloy [13], EDD steel [14], gas cylinder steel [15]. Also, different cup shapes such as pyramidal [2, 16], rectangular [3, 17] and cone [4, 18] were fabricated. In recent years, single point incremental forming (SPIF) is being used to fabricate variety of shapes using simple tooling without dies. In SPIF process (figure 1), the sheet material is clamped along its edges and a hemispherical headed tool is moved along a predefined geometrical path so that it deforms the sheet locally along the path. The important process parameters, which influence the SPIF process capability, are tool diameter, step depth, feed rate, rotational speed of the spindle, sheet thickness, lubrication and tool path [19]. It was observed that the strain paths are linear in the first stage and highly non-linear in the subsequent stages [20].

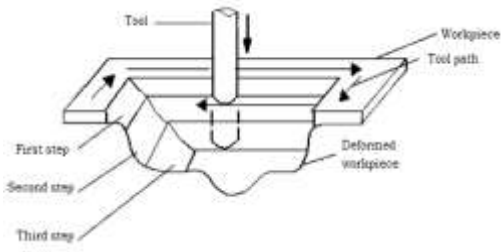

Figure 1: ***Single point incremental forming.***

ISSN: 2277-9655
Impact Factor: 4.116

The present work was to study the formability of truncated pyramidal cups of AA1050 alloy using SPIF. For this purpose the design of experiments was executed as per Taguchi technique. The process parameters of SPIF were sheet thickness, step depth, tool radius and coefficient of friction. The formability was evaluated using finite element method.

2. FINITE ELEMENT MODELING

In the present work, ABAQUS (6.14) software code was used for the numerical simulation of SPIF process to fabricate truncated pyramidal cups. the material was AA1050 alloy. The SPIF process parameters were chosen at three levels as summarized in table 1. The orthogonal array (OA), L9 was preferred to carry out experimental and finite element analysis (FEA) as given in table 2.

Table 1: Process parameters and levels

Factor	Symbol	Level–1	Level–2	Level–3
Sheet thickness, mm	A	1.0	1.2	1.5
Step depth, mm	B	0.50	0.75	1.00
Tool radius, mm	C	4.0	5.0	6.0
Coefficient of friction	D	0.05	0.10	0.15

Table 2: Orthogonal Array (L9) and control parameters

Treat No.	A	B	C	D
1	1	1	1	1
2	1	2	2	2
3	1	3	3	3
4	2	1	2	3
5	2	2	3	1
6	2	3	1	2
7	3	1	3	2
8	3	2	1	3
9	3	3	2	1

The sheet and tool geometry were modeled as deformable and analytical rigid bodies, respectively, using ABAQUS. they were assembled as frictional contact bodies. The sheet material was meshed with S4R shell elements (figure 2a). The fixed boundary conditions were given to all four edges of the sheet. as shown in figure 2b. The boundary conditions for tool were x, y, z linear movements and rotation about the axis of tool. True stress-true strain experimental data were loaded in the tabular form as material properties [21]. The tool path geometry was generated using CAM software [22] was imported to the ABAQUS as shown in figure 3. The elastic-plastic deformation analysis was carried out for the equivalent stress, strain and strain rates and thickness variation.

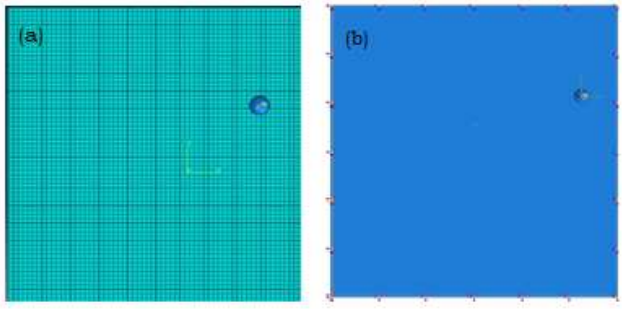

Figure 2: ***Finite element modeling: (a) mesh generation and (b) boundary conditions.***

ISSN: 2277-9655
Impact Factor: 4.116

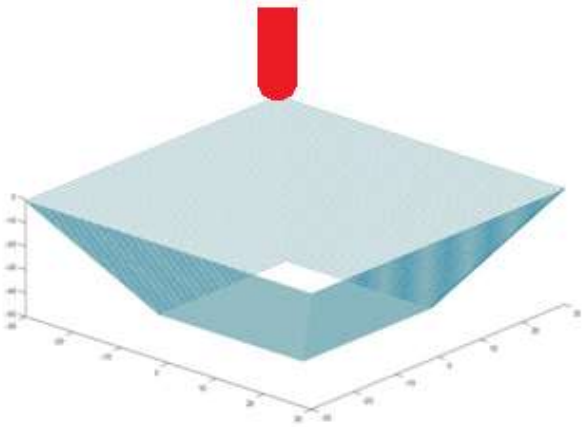

Figure 3: ***Tool path generation.***

3. RESULTS AND DISCUSSION

The results obtained from the elastic-plastic deformation analysis are discussed in the following sections. The Fisher's test was confirmed to accept all the parameters (A, B, C and D) at 90% confidence level. Hence, the process parameters which had an absolute Fisher's ratio larger than 3.4579 were believed to influence the average value for the forming characteristic under null hypothesis, parameters which had Fisher's ratio less than 3.457 were believed to have no effect on the average.

3.1 Influence of process parameters on effective stress

Table – 3 gives the ANOVA (analysis of variation) summary of effective stress data. The percent contribution specifies that tool radius, C contributes 39.87%, coefficient of friction, D accords 36.15%, step depth, B presents 15.07% and sheet thickness, A bequests of total variation on the effective stress (von Mises stress).

Table 3: ANOVA summary of the effective stress.

Source	Sum 1	Sum 2	Sum 3	SS	v	V	F	P
A	495.2	496	500.8	6.1075	1	6.1075	2444	8.87
B	500	492.8	499.2	10.3775	1	10.3775	4152	15.07
C	496.8	504	491.2	27.4475	1	27.4475	10980	39.87
D	492	504	496	24.8875	1	24.8875	9956	36.15
e				0.01	4	0.0025	1	0
T	1984	1996.8	1987.2	68.83	8			100

Note: *SS is the sum of square, v is the degrees of freedom, V is the variance, F is the Fisher's ratio, P is the percentage of contribution and T is the sum squares due to total variation.*

Figure 4 presents the influence of SPIF process parameters von Mises stress induced in AA1050 alloy. The von Mises stress was increased with increase of sheet thickness (figure 4a). The thickness of sheet definitely affects the force that need to apply for a given amount of elongation. Figure 4b describes the effective stress as a function of step depth. The effective stress was very low for the step size of 0.75 mm. The effective stress was high for tool radius of 5 mm as showed in figure 4c. The effective stress was found to be maximum for the coefficient of friction at 0.1. Either above or below of this value, the von Mises stress was low.

The principal stresses S_{11}, S_{22} and shear stress S_{12} are shown in figure 5, 6 and 7 respectively. The compressive stresses induced in the sheet are higher in number than the tensile stresses. The deformation based on compression for the strain less than 3.0 and it is tensile for the strain greater than 3.0. The shear stress developed in the blank sheet is nearly 60% -70% of S_{11}.

ISSN: 2277-9655
Impact Factor: 4.116

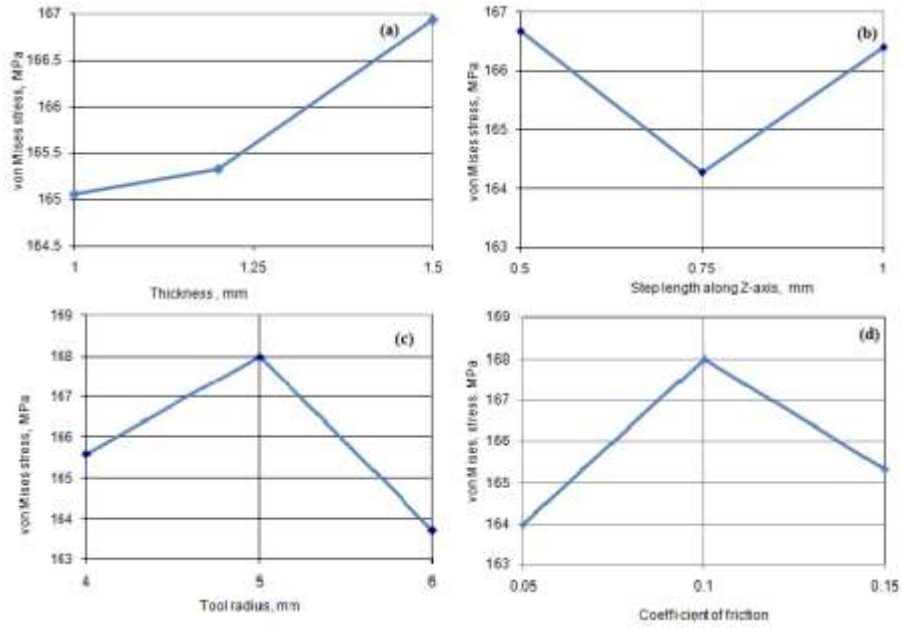

Figure 4: Influence of process parameters on von Mises stress.

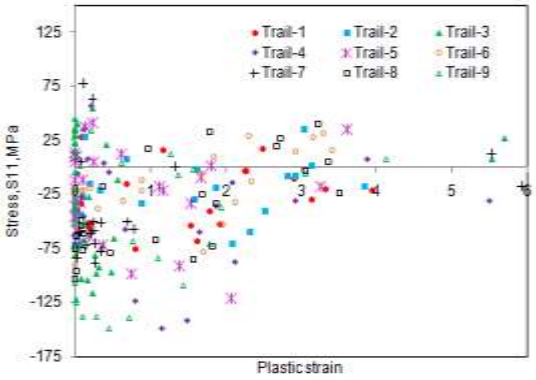

Figure 5: Effect of process parameters on S11.

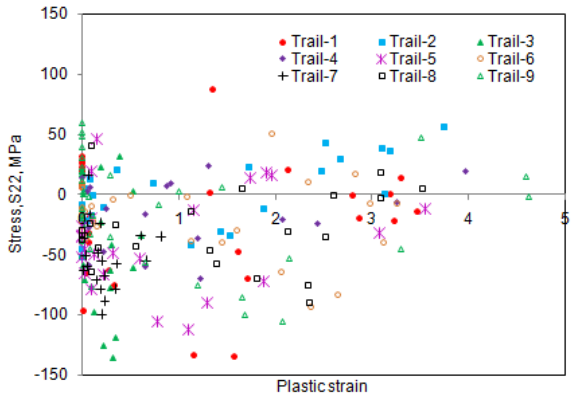

Figure 6: Effect of process parameters on S22.

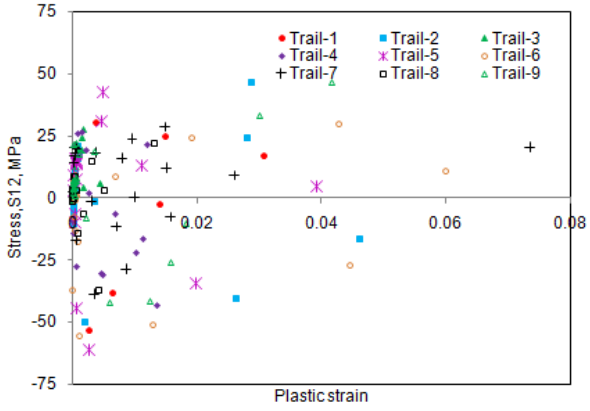

Figure 7: Effect of process parameters on S12

For the trials 1, 2 and 3, the von Mises stresses are, respectively, 164 MPa, 168 MPa and 163 MPa. For the trials 4, 5 and 6, the von Mises stresses are, respectively, 168 MPa, 160 MPa and 168 MPa. For the trials 7, 8 and 9, the von Mises stresses are, respectively, 168 MPa, 165 MPa and 168 MPa. The ultimate tensile strength of AA1050-H18 alloy is 160 MPa which is nearer for trials 3 and 5 (figure 8) .

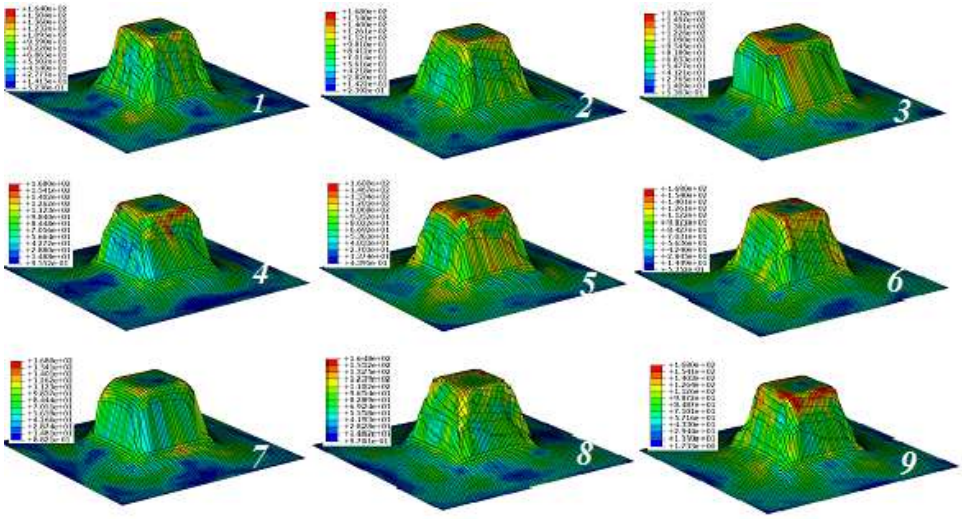

Figure 8: Raster images of von Mises stress in the cups.

3.2 Influence of parameters on strain rate:

The ANOVA summary of the strain rate is given in Table 4. The percent contribution column establishes the major contributions 43.47%, 31.41%, 17.16% and 7.97% of step depth, coefficient of friction, sheet thickness and tool radius, respectively, towards variation in the strain rate.

Table 4: ANOVA summary of the strain rate

Source	Sum 1	Sum 2	Sum 3	SS	v	V	F	P
A	10.97	10.737	15.405	4.61	1	4.61	11162.23	17.16
B	17.08	10.928	9.097	11.68	1	11.68	28280.87	43.47
C	11.35	11.313	14.441	2.14	1	2.14	5181.59	7.97
D	8.68	15.781	12.645	8.44	1	8.44	20435.84	31.41
e				-0.00165	4	-0.00041	1	0
T	48.09	48.759	51.588	26.87	8			100

The strain rate was increased with increase of sheet thickness and tool radius (figure 9a). The sheet thickness is the representative of the material availability for plastic deformation. Larger the thickness higher the availability of material for the plastic deformation. The strain rate was decreased with increase of step depth as shown in figure 9b. The magnitude of the step (Δz) down that the tool made after each pass is an important parameter which had an effect on the strain rate which depends upon the elastic-plastic deformation of sheet. For smaller step size local deformation plays an important role than stretching. As the tool radius increases, the area under the tool exposed to the plastic deformation also increases. Hence, increase in tool radius enhances the strain rate as shown in figure 9c. As observed from figure 9d, the strain rate was found to be high for coefficient of friction of 0.1. The cup formation depends on the shear stress developed during the plastic deformation of sheet material. The frictional shear stress is directly proportional to the coefficient of friction as per Coulomb's law of friction ($\tau = \mu F_n$, where F_n is the normal pressure). When the frictional shear stress, reaches the limiting shear stress of the sheet material, the material undergoes plastic deformation. From this point the frictional shear stress does not increase and has the value of the

ISSN: 2277-9655
Impact Factor: 4.116

limiting shear stress and thereby limiting the coefficient of friction [16, 17]. Therefore, at each contact spot of tool with sheet, the local strain determines the friction. A smaller length strain implies that the blank has stretched.

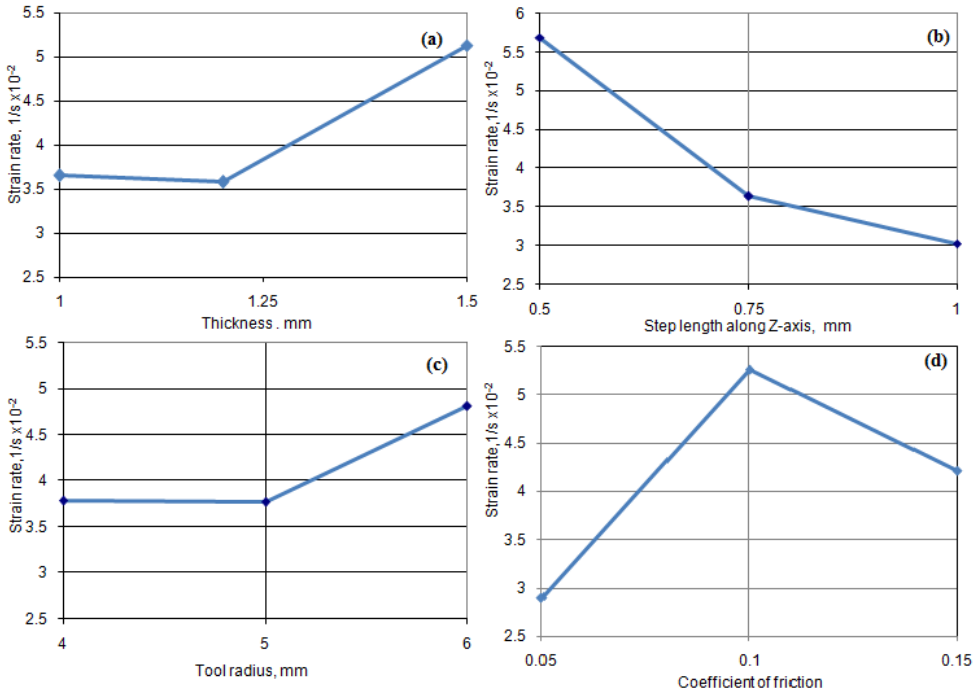

Figure 9: Influence of process parameters on strain rate.

3.3 Influence of parameters on thickness reduction

The ANOVA summary of the thickness reduction is given in Table 5. In the decreasing order of contribution, coefficient of friction, tool radius, step depth and sheet thickness accord, respectively, 59.70%, 31.82%, 6.09% and 2.36% towards variation in the thickness reduction.

Table 5: ANOVA summary of the thickness reduction

Source	Sum 1	Sum 2	Sum 3	SS	v	V	F	P
A	223.52	227.33	226.82	2.85	1	2.85	669.06	2.36
B	223.36	229.65	224.66	7.33	1	7.33	1720.76	6.09
C	231.89	228.40	217.37	38.29	1	38.3	8991.17	31.82
D	237.69	221.84	218.14	71.857	1	71.85	16867.25	59.7
e				0.017	4	0.0043	1	0
T	916.46	907.21	887.00	120.33	8			100

The major process parameters which influence the reduction of sheet thickness, are coefficient of friction and tool radius (figure 10). The reduction of sheet thickness was decreased with increase tool radius as shown in figure 10c. As mentioned earlier that the strain rate of the sheet increases with tool radius, the deduction in thickness is quiet obvious with increase of tool radius as per the conservation of volume in the forming processes. The cup formation process depends upon the shear stress induced in the sheet material. the shear stress is directly proportional to the coefficient of friction. Hence, the thickness reduction increases with increase of shear stress / coefficient of friction (figure 10d). The reduction of thickness was considered at the center-line of the deformed cup as shown in figure 11a. As observed from figures 11b-d, the majority of thickness reduction takes place in the walls of the cup but not in the flange or bottom of the cup. The elements located at the mid regions of the walls are elongated higher than those present at the top and bottom of the cup walls.

ISSN: 2277-9655
Impact Factor: 4.116

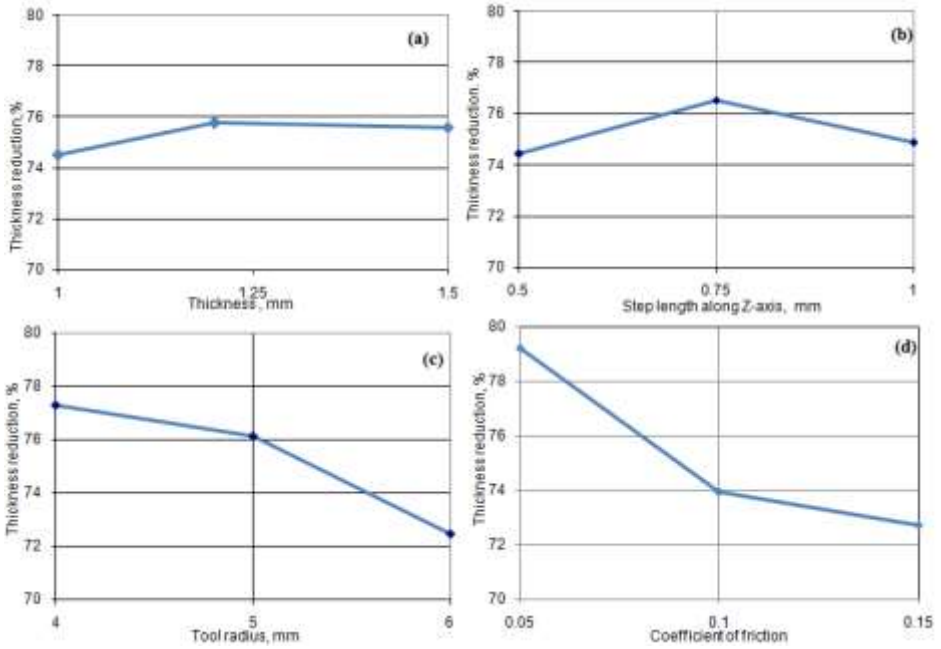

Figure 10: Influence of process parameters on thickness reduction.

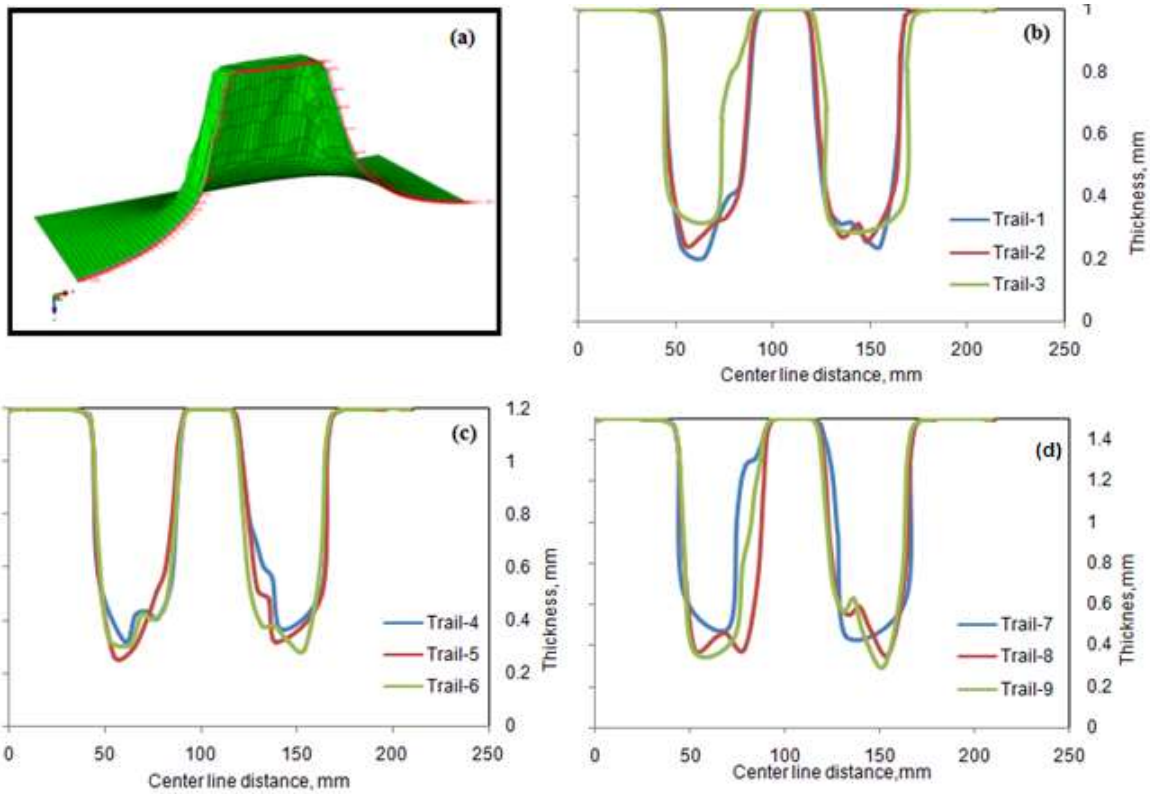

Figure 11: Location of thickness reduction in the deformed cup (a) and effect of process parameters on thickness reduction (b, c, d).

ISSN: 2277-9655
Impact Factor: 4.116

3.4 Formability of SPIF process

The formability diagrams of the cups are shown in figures 12a-c. During initial stages of SPIF, the shear and compressive stresses were dominating the formability of truncated pyramidal cups of AA1050 alloy. At later stages of plastic deformation the tension is highly predominant resulting the stretching sheet. For the trials 3 and 5 the formability limit diagram falls within the region of deep drawing process as compared with figure 12d. For the rest of trials, the formability limit diagrams fall within the region of failure due to uniaxial tension.

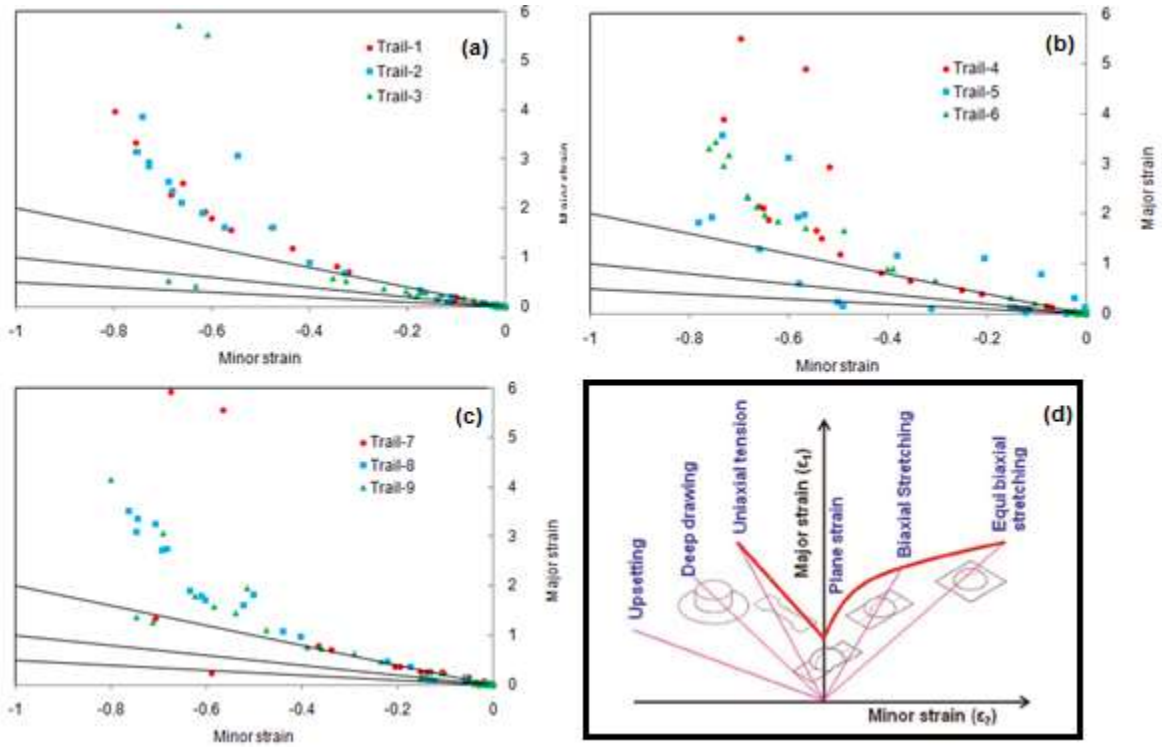

Figure 12: Forming limit diagrams (a)for trials 1, 2, 3 (b) for trials 4, 5, 6 (c) for trials 7, 8, 9 (d) Forming limit diagram of deep drawing process.

4. CONCLUSION

The major SPIF process parameters which influence the formability of truncated pyramidal cups of AA1050-H18 alloy were coefficient of friction and tool radius. The optimal process parameters could be sheet thickness of 1.5 mm, step depth of 0.5 mm, tool radius of 4.0 mm and coefficient of friction of 0.05.

ACKNOWLEDGEMENTS

The author acknowledges with thanks University Grants Commission (UGC) – New Delhi for sectioning R&D project.

REFERENCES

[1] A. C. Reddy, "Homogenization and Parametric Consequence of Warm Deep Drawing Process for 1050A Aluminum Alloy:Validation through FEA," International Journal of Science and Research, vol. 4, no.4, pp. 2034-2042, 2015.
[2] K. Chandini and A. C. Reddy, "Finite Element Analysis of Warm Deep Drawing Process for Pyramidal Cup of AA1070 Aluminum Alloy," International Journal of Advanced Research, vol. 3, no. 6, pp. 1325-1334, 2015.
[3] B. Yamuna and A. C. Reddy, "Finite Element Analysis of Warm Deep Drawing Process for Conical Cup of AA1080 Aluminum Alloy," International Journal of Advanced Research, vol. 3, no. 6, pp. 1309-1317, 2015.
[4] T. Srinivas and A. C. Reddy, "Finite Element Analysis of Warm Deep Drawing Process for Rectangular Cup of AA1100 Aluminum Alloy," International Journal of Advanced Research, vol. 3,no. 6, pp. 1383-1391, 2015.

[5] A. C. Reddy, "Parametric Optimization of Warm Deep Drawing Process of 2014T6 Aluminum Alloy Using FEA," International Journal of Scientific & Engineering Research, vol. 6, no. 5, pp.1016-1024, 2015.
[6] A. C. Reddy, "Finite Element Analysis of Warm Deep Drawing Process for 2017T4 Aluminum Alloy: Parametric Significance Using Taguchi Technique," International Journal of Advanced Research, vol. 3, no. 5, pp. 1247-1255, 2015.
[7] A. C. Reddy, "Parametric Significance of Warm Drawing Process for 2024T4 Aluminum Alloy through FEA," International Journal of Science and Research, vol. 4, no. 5, pp. 2345-2351, 2015.
[8] A. C. Reddy, "Formability of High Temperature and High Strain Rate Superplastic Deep Drawing Process for AA2219 Cylindrical Cups," International Journal of Advanced Research, vol. 3,no. 10, pp. 1016-1024, 2015.
[9] A. C. Reddy, "High temperature and high strain rate superplastic deep drawing process for AA2618 alloy cylindrical cups," International Journal of Scientific Engineering and Applied Science, vol. 2, no. 2, pp. 35-41, 2016.
[10] A. C. Reddy, "Practicability of High Temperature and High Strain Rate Superplastic Deep Drawing Process for AA3003 Alloy Cylindrical Cups," International Journal of Engineering Inventions, vol. 5, no. 3, pp. 16-23, 2016.
[11] A. C. Reddy, "Suitability of High Temperature and High Strain Rate Superplastic Deep Drawing Process for AA5052 Alloy," International Journal of Engineering and Advanced Research Technology, vol. 2, no.3, pp. 11-14, 2016.
[12] A. C. Reddy, "High temperature and high strain rate superplastic deep drawing process for AA5049 alloy cylindrical cups," International Journal of Engineering Sciences & Research Technology, vol. 5, no.2, pp. 261-268, 2016.
[13] A.C. Reddy, "Finite element analysis of reverse superplastic blow forming of Ti-Al-4V alloy for optimized control of thickness variation using ABAQUS," Journal of Manufacturing Engineering, vol. 1, no.1, pp.6-9, 2006.
[14] A. C. Reddy, T. K. K. Reddy, M.Vidya Sagar, "Experimental characterization of warm deep drawing process for EDD steel," International Journal of Multidisciplinary Research & Advances in Engineering, vol. 4, no.3, pp.53-62, 2012.
[15] A. C .Reddy, "Evaluation of local thinning during cup drawing of gas cylinder steel using isotropic criteria," International Journal of Engineering and Materials Sciences, vol. 5, no.2, pp.71-76, 2012.
[16] A. C. Reddy, "Formability of Warm Deep Drawing Process for AA1050-H18 Pyramidal Cups," International Journal of Science and Research, vol. 4, no.7, pp. 2111-2119, 2015.
[17] A. C. Reddy, "Formability of Warm Deep Drawing Process for AA1050-H18 Rectangular Cups," International Journal of Mechanical and Production Engineering Research and Development, vol. 6, no.4, pp. 85-97, 2015.
[18] A. C. Reddy, "Formability of superplastic deep drawing process with moving blank holder for AA1050-H18 conical cups," International Journal of Research in Engineering and Technology, vol. 4, no.8, pp. 124-132, 2015.
[19] J. Jeswiet, F. Micari, G. Hirt, A. Bramley, J. Duflou, J. Allwood, "Asymmetric single point incremental forming of sheet metal," CIRP Annals-Manufacturing Technology, vol. 54, no.2, pp.88-11, 2005.
[20] M. B. Silva, M. Skjoedt, N. Bay, P. A. F. Martins, "Multistage Single Point Incremental Forming" In proceedings of Congress on Numerical Methods in Engineering APMTAC, Portugal, 2011.
[21] Chennakesava R. Alavala, "Finite element methods: Basic Concepts and Applications, PHI Learning Pvt. Ltd., 2008.
[22] Chennakesava, R. Alavala, "CAD/CAM: Concepts and Applications," PHI Learning Pvt. Ltd, 2008:
[23] H. Lubbinge, R. T. Haar, D. J. Schipper, "The Influence of Plastic Bulk Deformation on Surface Roughness and Frictional Behavior during Deep Drawing Processes," In Proceedings of the Leeds/Lyon Conference, Lyon, 1995.
[24] J. F. Lin, L. Y. Wang, and T. Huang, "Friction in deep drawing of aluminium sheet," Wear, vol. 156, pp. 189-199, 1992.